Barrier Layers Observed in a High-resolution Model in the Eastern Tropical Pacific

F. M. Bingham[1], Z. Li[2], S. Katsura[3], J. Sprintall[3]

[1]University of North Carolina Wilmington, Center for Marine Science, Wilmington, NC, USA.
[2]California Institute of Technology, Jet Propulsion Laboratory, Pasadena, CA, USA.
[3]Scripps Institution of Oceanography, University of California, San Diego

Corresponding author: Frederick M. Bingham (binghamf@uncw.edu)

Key Points:

- Salinity barrier layers (BLs) in the eastern tropical North Pacific are characterized using a high-resolution numerical model
- BLs are associated with surface salinity fronts which tilt towards the fresh side at their base
- Vertical circulation combined with surface divergence and convergence are proposed as an additional formation mechanism for BLs in this region.

Abstract

Salinity barrier layers (BLs) are common in the eastern tropical North Pacific (ETP) and may play an important role in regulating the transfer of heat, momentum and freshwater across the ocean surface. This study examines BLs in the ETP in the region of the SPURS-2 (Salinity Processes in the Upper ocean Regional Studies – 2) field campaign. We utilize a high-resolution numerical model to study BLs and their relationship to frontal features and small-scale ocean variability, focusing on two specific events. One is associated with a large outbreak of BL presence near 7°N along 125°W. The other is a relatively isolated but persistent BL that forms near 13°N, again along 125°W. In both cases we find that the BL is proximate to a salinity frontal feature in which isohalines tilt toward the fresh side of the front at its base. The BLs studied are associated with divergent flow at the surface on the fresh side of the front and convergent flow on the salty side. Tilting of the front is invoked to explain this, with an additional mechanism involving a vertical circulation which causes the base of the front to tilt preferentially.

Plain Language Summary

Salinity barrier layers (BLs) are common in the eastern tropical North Pacific (ETP) and may play an important role in regulating the transfer of heat, momentum and freshwater across the ocean surface. This study examines BLs in the ETP in the region of the SPURS-2 (Salinity Processes in the Upper ocean Regional Studies – 2) field campaign. We utilize a high-resolution numerical model to study BLs and their relationship to small-scale ocean variability, focusing on two specific events. One is associated with a large outbreak of BL presence near 7°N along 125°W. The other is a relatively isolated but persistent BL that forms near 13°N, again along 125°W. In both cases we find that the BL is proximate to a horizontal salinity front which tilts toward the fresh side at its base. The BLs studied are associated with divergent flow at the surface on the fresh side of the front and convergent flow on the salty side. Tilting of the front is invoked to explain this, with an additional mechanism involving a vertical circulation which causes the base of the front to tilt preferentially.

1 Introduction

Barrier layers (BLs) are areas in the upper ocean where the surface mixed layer as defined by temperature is greater than that as defined by density due to an intrusion of salty water at the base of the mixed layer. They have been observed in the ocean since their discovery about 30 years ago (Godfrey and Lindstrom, 1989; Lukas and Lindstrom, 1991). BLs have been found in a diverse set of contexts (Sprintall and Tomczak, 1992; de Boyer Montegut et al., 2007), most especially in the tropics and at high latitudes, and are an important part of upper ocean dynamics in these areas (Roemmich et al., 1994; Vialard and Delecluse, 1998a). In the tropics in particular, they are thought to modulate air-sea interaction by creating a layer of insulating stratification, which can magnify the impact of heat and/or freshwater flux at the surface (Maes et al., 2002; Maes et al., 2005). They also act to suppress entrainment cooling at the base of the mixed layer, since water in the mixed layer is at the same temperature as water below it (Godfrey and Lindstrom, 1989; Vialard and Delecluse, 1998b).

Katsura and Sprintall (2020; henceforth “KS20”) have shown that BLs are ubiquitous in the eastern tropical Pacific (ETP) under the intertropical convergence zone (ITCZ). Their presence is highly seasonal, with maximum likelihood and thickness in the summer and fall.

KS20 attribute the common presence of BLs in this region to convergent Ekman transport driven by wind stress curl. The Ekman convergence creates mixed layer salinity fronts, which then tilt due to instability and shear between the surface and the base of the mixed layer. This process of tilting was first proposed by Cronin and McPhaden (2002; henceforth "CM02") as one potential mechanism for BL formation. KS20's conclusion is congruent with Sato et al., (2004), Sato et al. (2006), and Katsura et al. (2015), who all emphasized the role of sharp small-scale salinity fronts and subduction of high salinity water in the tropical and subtropical ocean. However, the conclusions of KS20 and those of Sato et al. (2006) are based on Argo data which are relatively sparse in space and time. In particular, KS20 cannot co-locate the BLs relative to the concurrent position of the North Equatorial Counter Current (NECC) or any property front associated with the circulation system, nor do they shed any light on what specific dynamics may be occurring at the front associated with BL formation. Indeed, it is difficult to obtain the direct measurements of the 3-dimensional circulation and air-sea interaction that are needed to determine the mechanisms responsible for BL formation using an *in situ* dataset.

Katsura et al. (2020) looked in more detail at BL and temperature inversion formation using the higher resolution SPURS-2 (Salinity Processes in the Upper ocean Regional Studies – 2) in situ dataset. They reached a similar conclusion as KS20, that BLs form as a result of tilting of mixed layer fronts. Additionally, they surmise that BLs form in a patchy and intermittent manner on fast time scales and that surface geostrophic flow and Ekman flow play important roles in causing the tilting of frontal isohalines - where BL formation occurs.

The ETP is the location of the seasonal extension of the ETP fresh pool (Alory et al., 2012; Melnichenko et al., 2019), a low surface salinity feature which extends westward from the coast of Central America. It reaches its maximum extent in the October/November period, reaching out to ~160°W, as defined by the 34 isohaline, with minimum extent in January/February at ~125°W. Its meridional extent, again defined by the 34 isohaline, is about 10° in the mean between about 5 and 15°N (Guimbard et al., 2017; Fiedler and Talley, 2006). At the southern edge of this fresh pool extension is a surface front separating the relatively fresh eastern Pacific water from higher salinity surface water found at the equator. This front forms in January near ~3°N, migrates to the north over the course of the year, and dissipates in the months of January-February after reaching a maximum latitude of about 12°N (Yu, 2015). In the October-November period it is generally found around 6-7°N, which is one location where the present study will focus.

The ETP was the location, in 2016-2017, of the SPURS-2 field campaign (Lindstrom et al. (2019) and references therein). SPURS-2 was carried out to study the impact of rainfall on the upper ocean salinity field, and the creation of the Pacific basin-wide low sea surface salinity (SSS) feature (e.g. Schanze et al., 2010). Associated with the field campaign, there was an effort to model the dynamics in a regional ocean model based on the Regional Ocean Modeling System (ROMS; Li et al., 2019, henceforth "Li19"; Shchepetkin and McWilliams 2011). Using this numerical model, we can focus in on the mechanisms responsible for BL formation, and examine how or whether the BL formation is related to 3-dimensional frontal structures and their temporal evolution. As stated by Tanguy et al. (2010), a complete understanding of BL formation requires information "on the 3-dimensional structure of the upper ocean, T, S, velocity, vertical shear, local surface forcing and turbulent mixing". BL formation in numerical models has been studied by Veneziani et al. (2014) in the South Atlantic, also using ROMS, though configured specifically for that different region. They emphasized the importance of advection, and, importantly, of the influence from submesoscale processes and their impact on vertical transport of heat and salt.

In this paper, we study BL formation in a couple of individual events within the high-resolution ROMS daily output. The ROMS output displays BLs in the ETP, which can be related to surface circulation, surface convergence, salinity, winds and freshwater forcing from the atmosphere. By studying a couple of individual instances in detail, we can infer more broadly about how BLs relate to the dynamics of the ETP fresh pool and its seasonal extension across the Pacific.

2 Data and Methods

2.1 ROMS Simulation

The ROMS simulation uses data assimilation to constrain the large-scale and large mesoscale circulations as a method for more realistically reproducing BL formation. Li19 provide a description of the model, so the reader is referred there for more in depth details on the setup, forcing, validation, etc. The model is nested in three levels, 9 km, 3 km and 1 km (see Figure 2 in Li19). We use the 3 km, middle level, with daily average output. In the vertical, the model has 52 levels. To resolve effectively dynamical processes associated with the BL formation, there are 22 levels within top 100 m, with 2 m resolution at the surface, 5 m resolution at 50 m, and 10 m resolution at 100 m. The model covers the time period 1 February 2017 – 31 January 2018, whereas the SPURS-2 field campaign went from late August 2016 to early November 2017. Thus, the model and field campaign overlap for about 9 months of 2017 (Figure 1).

The atmospheric forcing for ROMS is derived from the 18 km resolution NCEP GFS (National Centers for Environmental Prediction Global Forecast System) operational atmospheric model output. A bulk flux formula (Fairall et al., 2003) is used to calculate the forcing. The inputs include 3-hourly atmospheric fields of 10-m wind speed and direction, net shortwave radiation, downward longwave radiation, 2 m air temperature, 2 m relative humidity, and precipitation. The 18 km resolution does not allow one to distinguish individual rain events and thus changes to SSS due to patchy and heavy rainfall associated with convective activity are not represented in the ROMS simulation.

The model assimilates a number of datasets. One of these is the monthly-average data from version 4 of the Met Office Hadley Centre ''EN'' series (Good et al., 2013). This monthly dataset constrains three-dimensional T/S fields on spatial scales larger than 400 km and thus is used to reduce model bias. Another assimilated dataset is the gridded AVISO (Archiving, Validation and Interpretation of Satellite Oceanographic data) sea surface height product. This product has a grid of 0.25°, but the effective resolution is about 300 km (Pujol et al., 2016). Satellite SST measurements from the Advanced Microwave Scanning Radiometer-2 (AMSR-2), a passive microwave radiometer flying on NASA's Aqua satellite, are also assimilated. The AMSR-2 SST has a resolution of 0.25°. Using the multi-scale scheme as described in Li et al (2015, 2019), the data assimilation is configured to primarily constrain eddies and circulation with spatial scales larger than 300 km. There are no SPURS-2 in situ observations assimilated in this 3 km model domain.

From the model output, we computed such quantities as divergence and vorticity. Isothermal layer depth (ILD) and mixed-layer depth (MLD) were determined using the method of deBoyer Montegut et al. (2007) with a potential temperature criterion of 0.2°C. BL thickness (BLT) is the difference between ILD and MLD when that difference is greater than zero. In the supporting information we include an animation of BLT within the model during the SPURS-2 period along with SSS (Animation S1). Thick BLs are often generated within eddies (e.g. 8-Feb – 20-Feb-2017 at 12.5°N,124°W) or across strong fronts (e.g. 12-May – 22-May-2017 at 13°N,125°W). These BLs can persist for days or weeks, or appear and disappear in a day or two (e.g. 31-July – 1-August-2017). BLs appear in the model output, but they are not generally as thick or persistent as those in the *in situ* data. This is evident through a comparison (Figure 1) between model output and observed T/S data from the SPURS-2 central mooring at (10°N,125°W) (Farrar, 2020; Farrar and Plueddemann, 2019). Note the ubiquitous presence of 20-30 m thick BLs in late summer and fall in the mooring data which are either absent or more sporadic in the ROMS simulation.

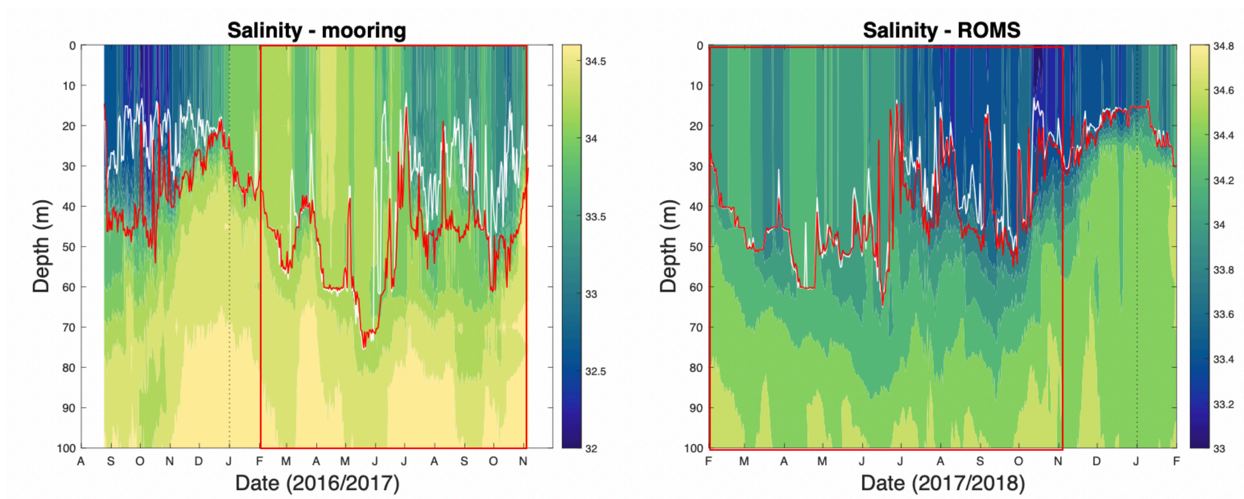

(a) (b)

Figure 1. Time series of salinity vs. depth observed at the SPURS-2 central mooring (Farrar, 2020) (a) and from the corresponding grid cell in the ROMS simulation (b). ILD is in white and MLD in red. The difference between them is the BLT. Color scales are at right for each panel, note different limits. Also note these two panels do not cover the same periods. Mooring salinity covers the period August 2016 – November 2017, whereas the ROMS salinity is computed over February 2017 – January 2018. A red box in each panel outlines the overlapping time period, February-November 2017.

3 Results

Animation S1 shows BLs appearing commonly throughout the model domain. They are often associated with frontal features (e.g. 11 January 2018 near 14.5°N,127°W), or found in the centers of low SSS-core eddies (e.g. 10-20 February 2017 near 12.5°N,123.5°W). They can persist for days, or pop up and disappear quickly (e.g. 31 July 2017). They can be isolated in time and space, or be ubiquitous throughout a large part of the domain shown (e.g. 29 June 2017).

Here we analyze two instances where thick BLs were observed in the ROMS simulation. One is associated with the presence of BLs in an extensive region of the ETP, whereas the other is a relatively isolated event in time and space. We use these events to illustrate the characteristics of BL formation in the model domain.

3.1 27-October-2017

On 27-October-2017 there is a very thick BL around 6-7°N from 126°W to 120°W (Animation S1). Indeed, much of the model domain south of 8°N on this date shows BLs that are >25 m thick. These thick BLs are associated with a SSS front that snakes through the region from (6°N,120°W) to (8°N,131°W). On 27-October the BL is centered at about 6.75°N, but is relatively thick from 6°N to 7.5°N along 125°W (Figure 2 right panel). What is clear from the SSS is the low salinity water spreading to the south during the prior two days. Water in the vicinity of the thick BL is much fresher on 27-October than the two previous days when no or minimal BLs existed.

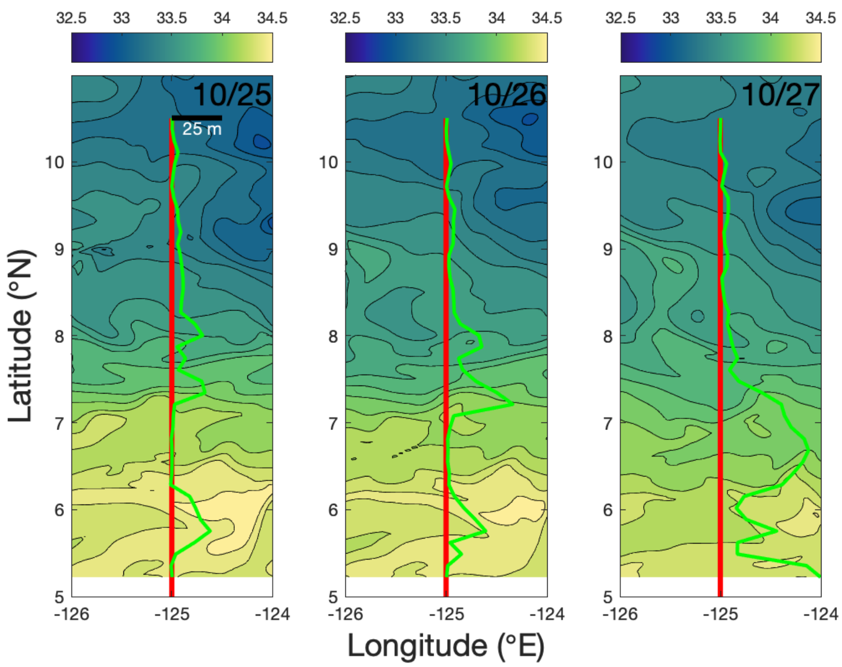

Figure 2. SSS from the ROMS domain on (left panel) 25, (center panel) 26 and (right panel) 27 October 2017. Color scale is at the top. Red line is along 125°W. The thick green line represents the BLT at 125°W at a given latitude, where zero BLT is the red line and 25 m BLT is indicated by the scale bar at 10.5°N in the left panel.

The ocean current vectors (Figure 3) on 27-Oct show water flowing southward throughout the entire domain. Clearly the thick BL of 27-Oct is associated with the sharply decreased SSS brought about by advection and the southward motion of a SSS front. A convergent feature is evident in the northern part of the region of thick BLs around 7°N (Figure 3 right panel). Just to the south of this convergent feature is an area of divergence near the center of the area of thick BL. This same convergent feature has migrated over the previous two days

202 when it is also associated with thick BLs, although not as thick as on 27 October (e.g. 7.2°N on
203 26 October). So thick BL formation appears to be associated with surface convergence and
204 divergence.

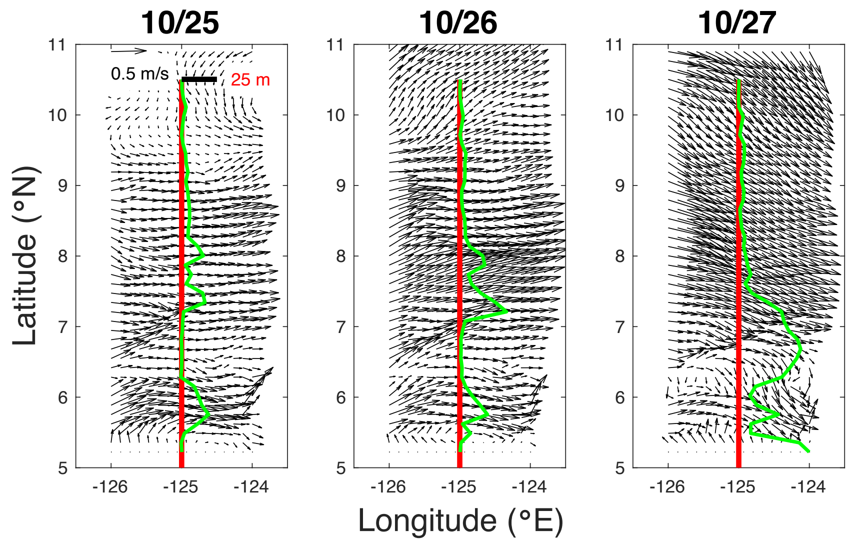

205

Figure 3. As in Figure 2, but for current velocity vectors. A scale arrow is at the top left in the left panel.

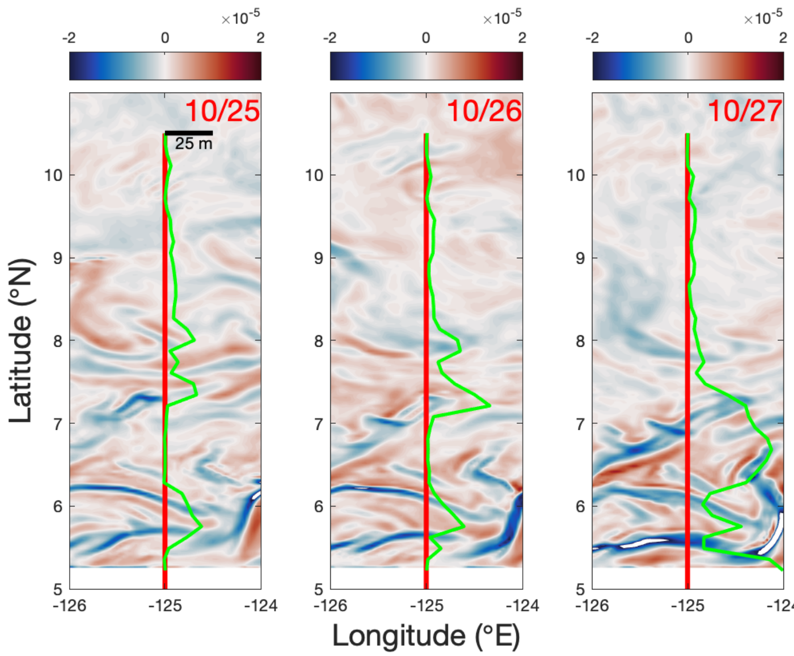

Figure 4. As in Figure 2, but for horizontal divergence. Color scale is at the top of each panel in units of s^{-1}.

The thick BLs on all three days are associated with areas of intense surface divergence and convergence culminating on 27 October (Figure 4 right panel). The thickest BLs are associated with surface divergence and there is some indication that surface convergence is associated with reduced BLT (e.g., 5.5°N and 6°N on 27 October). There are also places where thick BLs are associated with alternating surface convergence and divergence, for example around 6°N on 25 October and 7.25°N on 26 October.

The precipitation forcing the model is very small on 27 October and far removed from where the thick BLs are formed (Figure 5). An area of heavy precipitation is located at (7.75°N,125.5°W) on 26 October which may have had an influence on the thick BLs at 6.75°N the following day, though this is not obvious from the SSS shown in Figure 2.

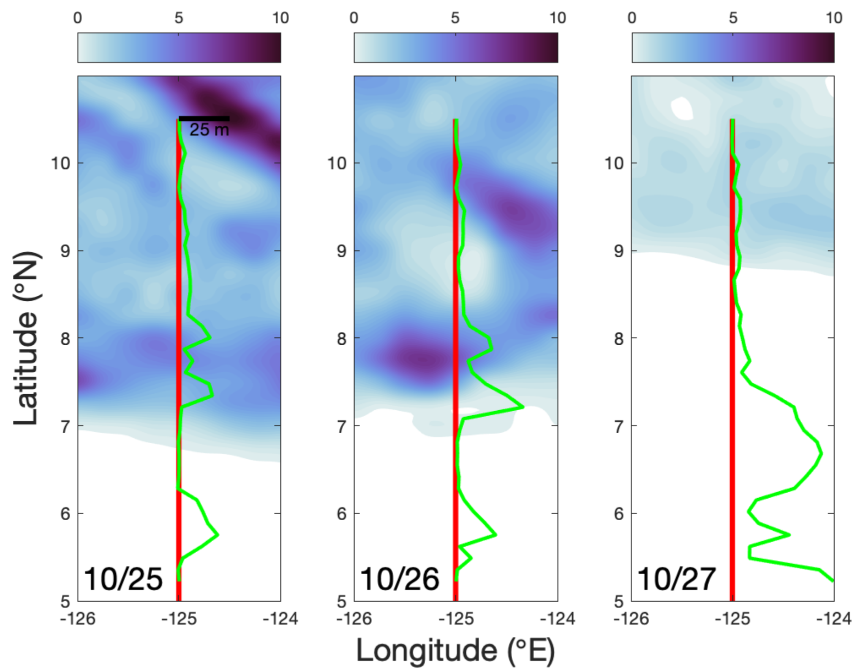

Figure 5. As in Figure 2, but for daily average precipitation rate. Color scale is at the top for each panel in units of mm hr^{-1}.

Wind speed undergoes a rapid change from 25-26 October to 27 October (Figure 6). On 27 October, the winds were nearly calm, whereas in the region of thick BL the winds were up to 8 m s^{-1} on the previous two days. The winds on 25-26 October were mainly out of the south (not shown). Perhaps the sudden change in the winds allowed low SSS water at the surface to drift southward after the change?

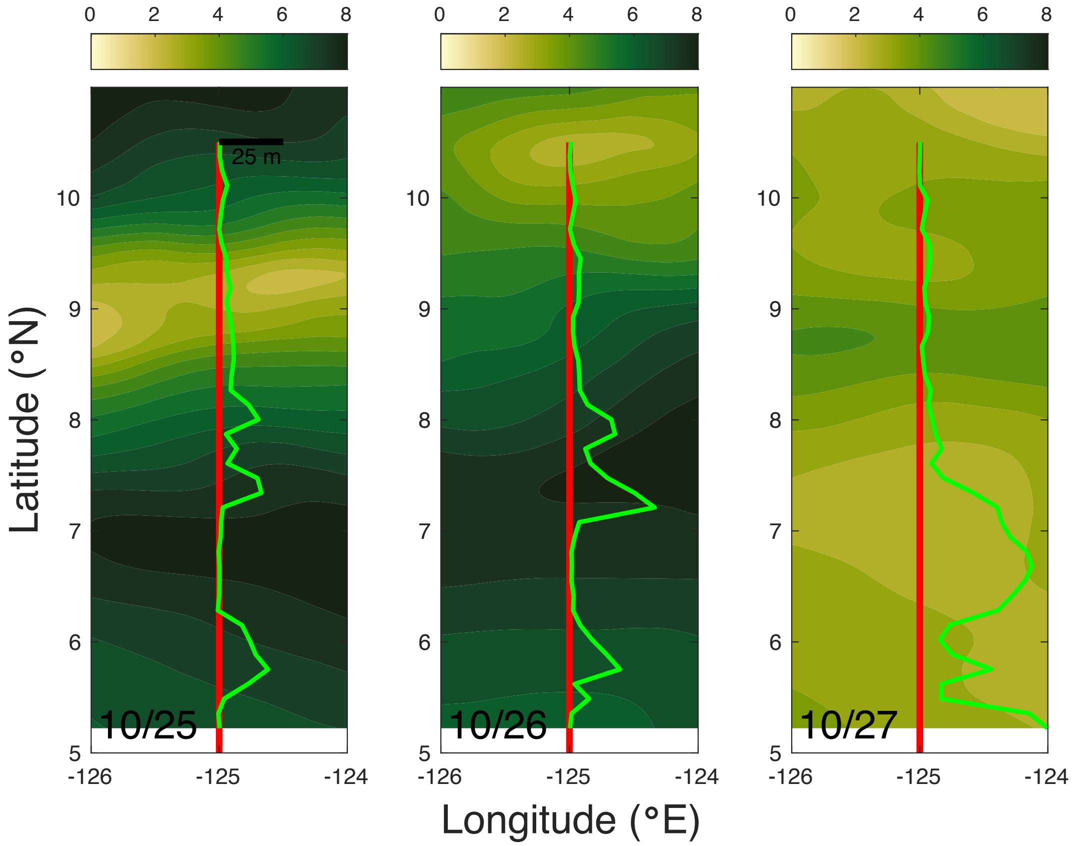

Figure 6. As in Figure 2, but for surface wind speed. Color scale is at the top for each panel in units of m s^{-1}.

A meridional section along 125°W (Figure 7) shows fresh surface water spreading across the area between 6 and 7°N and the generation of a thick BL. On 25 and 26 October, there is a thin BL between 7 and 8 °N. By 27-October, relatively fresh surface water had spread southward to around 6°N. This spreading occurred in the upper 20 m as evident in the large salinity difference shown in Figure 7d. The spreading left a thick BL between 6.25 and 7°N. South of there, between 26 and 27 October, the ILD shoaled from 60 to 30 m. What we see here is somewhat like the tilting of isohalines posited by CM02, but it is not exactly the same. In the main, the isohalines tilt during the days shown, but the tilting goes on mostly below 20 m depth. That is, the base of the isohalines tilts, but the upper part remains vertical. The salinity front at 7.5°N relaxes and spreads southward. CM02 implied that BLs are generated by current shear which causes the tilting (see their Figure 1). A complicating fact is that the zonal flow is much stronger than meridional. Perhaps in this case the tilting is not caused by cross-front vertical shear, but by some other mechanism.

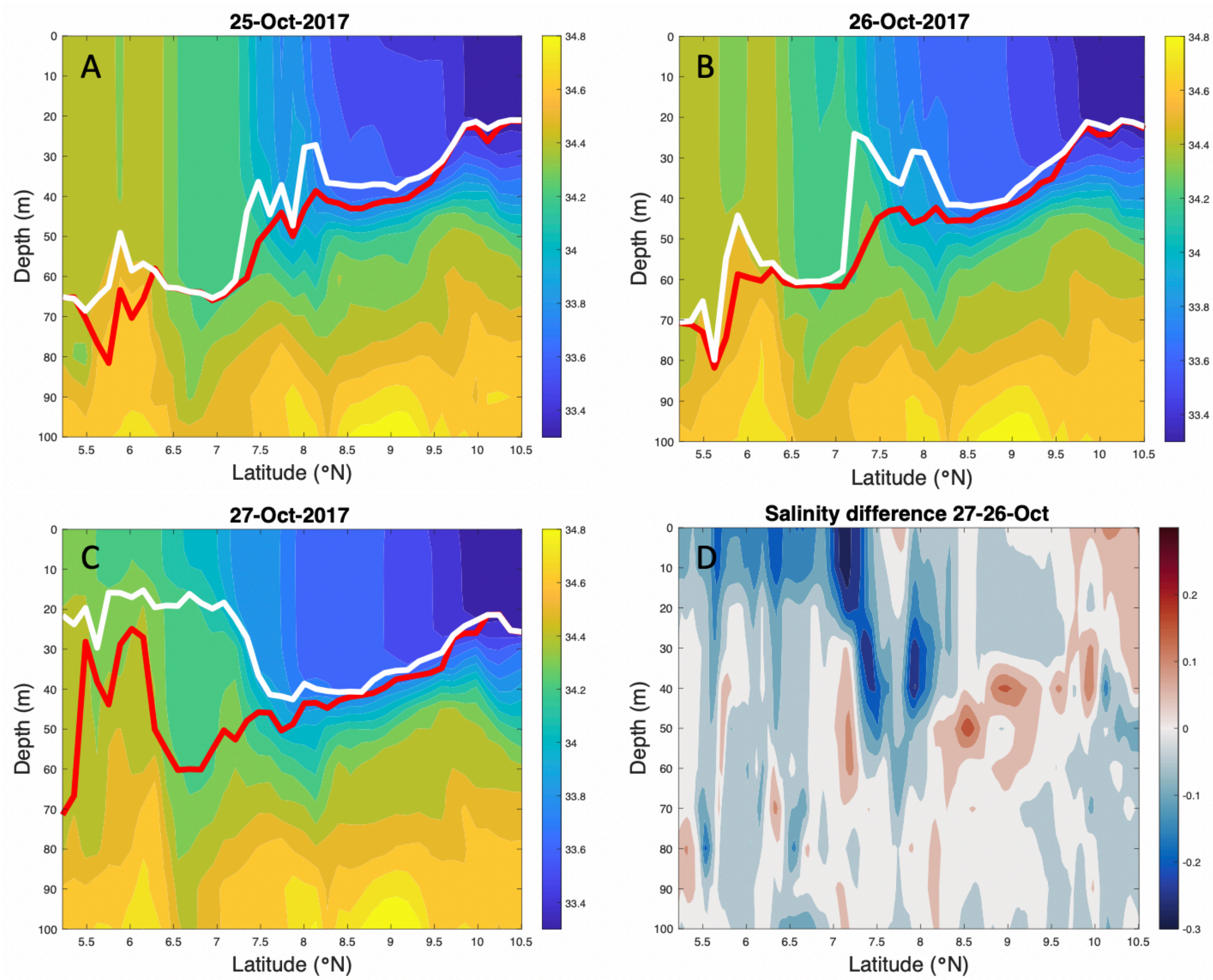

Figure 7. Salinity sections along 125°W for (a) 25 October, (b) 26 October and (c) 27 October. Color scales are at right. Thick red line is the ILD, while thick white line is the MLD. (d) Difference between panels (c) and (b).

October 2017 coincided with one of the two main SPURS-2 cruises. A uCTD section to ~250 m was obtained along 125°W from 10.5 to 5°N on 26-28 October (Figure 8). This uCTD section also showed that a thick BL existed, but it was much thicker (~50 m) and more extensive (from 9° to 6°N) than that produced in the ROMS output (Figure 7). There is as salinity front at the surface near 6.5°N. We also see the same configuration of the front, vertical isohalines at the surface and tilted ones below it as was observed for the model. The difference here is the that BL is much thicker in the uCTD data and the part of the water column with vertical isohalines much thinner. Katsura et al. (2020) show a similar section from a few days later, 3-5 November.

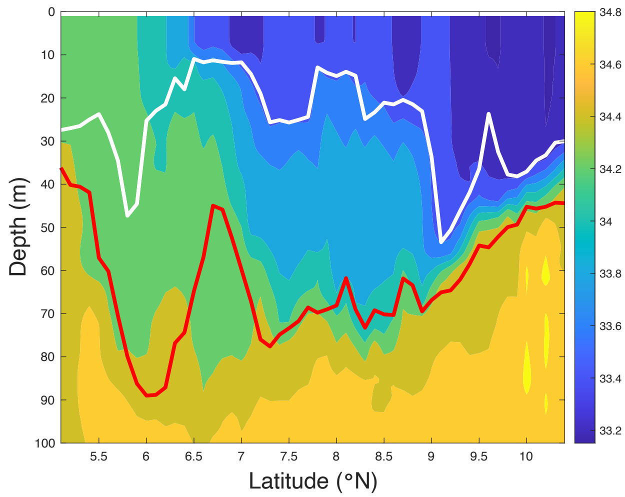

Figure 8. Salinity section from uCTD data (Sprintall, 2019a,b) along 125°W collected on the R/V Roger Revelle, 26-28 October 2017. Color scale is shown at right. Thick red line is the ILD, while thick white line is the MLD.

It is clear from Figures 3 and 4 that the presence of BLs is strongly related to surface horizontal divergence/convergence. Thus, because divergence and convergence are usually accompanied by vertical motion, it is likely related to vertical processes such as vertical flows, mixing and entrainment. The vertical velocity along 125°W (Figure 9) shows alternating bands of strong upward and downward flow in the mixed layer south of 7.5°N on 27 October. As expected, these bands are directly related to the maps of surface divergence (Figure 3), upward flow occurs where there is surface divergence and downward flow where there is convergence. The strong flow ceases at the base of the mixed layer, except for one band of downward flow at 5.6°N. For the most part, where the BL is thickest, the flow is upward. Where vertical velocity is minimal, north of 8°N, BLs are thin to non-existent. This pattern is repeated at 5.5-6°N and 7.5-8°N on the previous day (Figure 9a).

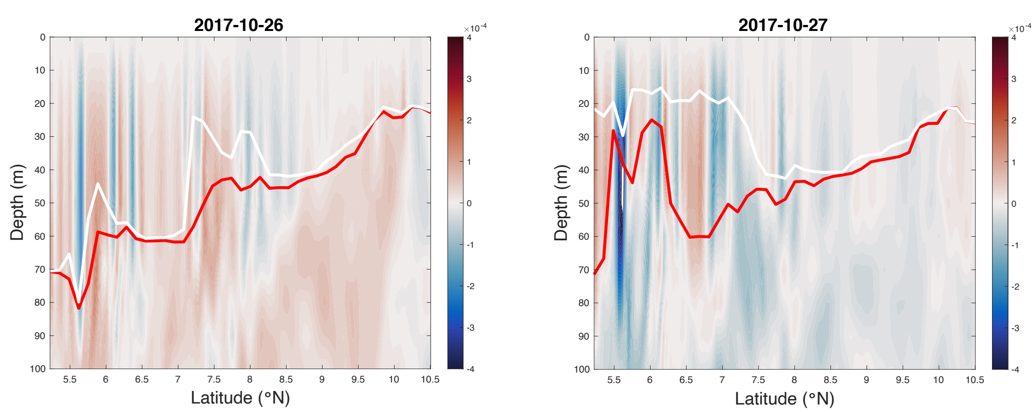

(a) (b)

Figure 9. Vertical velocity sections along 125°W for (a) 26 and (b) 27 October. Color scales (in m/s) are at right. Red colors are upward and blue downward. Thick red line is the ILD, while thick white line is the MLD.

3.2 7-26 May 2017

Between 7 and 26 May 2017, especially starting around 9 May, a BL developed across a north-south oriented front between 12 and 13°N near 125°W (Animation S1). This BL reached a maximum BLT of more that 25 m and persisted for almost three weeks within the front, eventually migrating northward to turn to an east-west orientation further north before dissipating by 30-May. The BL is clearly evident in the horizontal plan view (Figure 10a, see also Animation S2). Similar to 25-27 October 2017, there is tilting of isohalines (Figure 10b). The BL is situated on the low salinity side of the front at 125°W, with fresher water to the east. The front is tilted in the vertical, but not uniformly. All of the tilting occurs at the base of the front between 30 and 60 m depth, similar to that found in October 2017 (Figure 7b). The velocity field is highly convergent at the front (Figure 11 left panel), with the strongest convergence being at the front base at a depth of 60-70 m. Figures 10 strongly supports the CM02 tilting mechanism of BL formation.

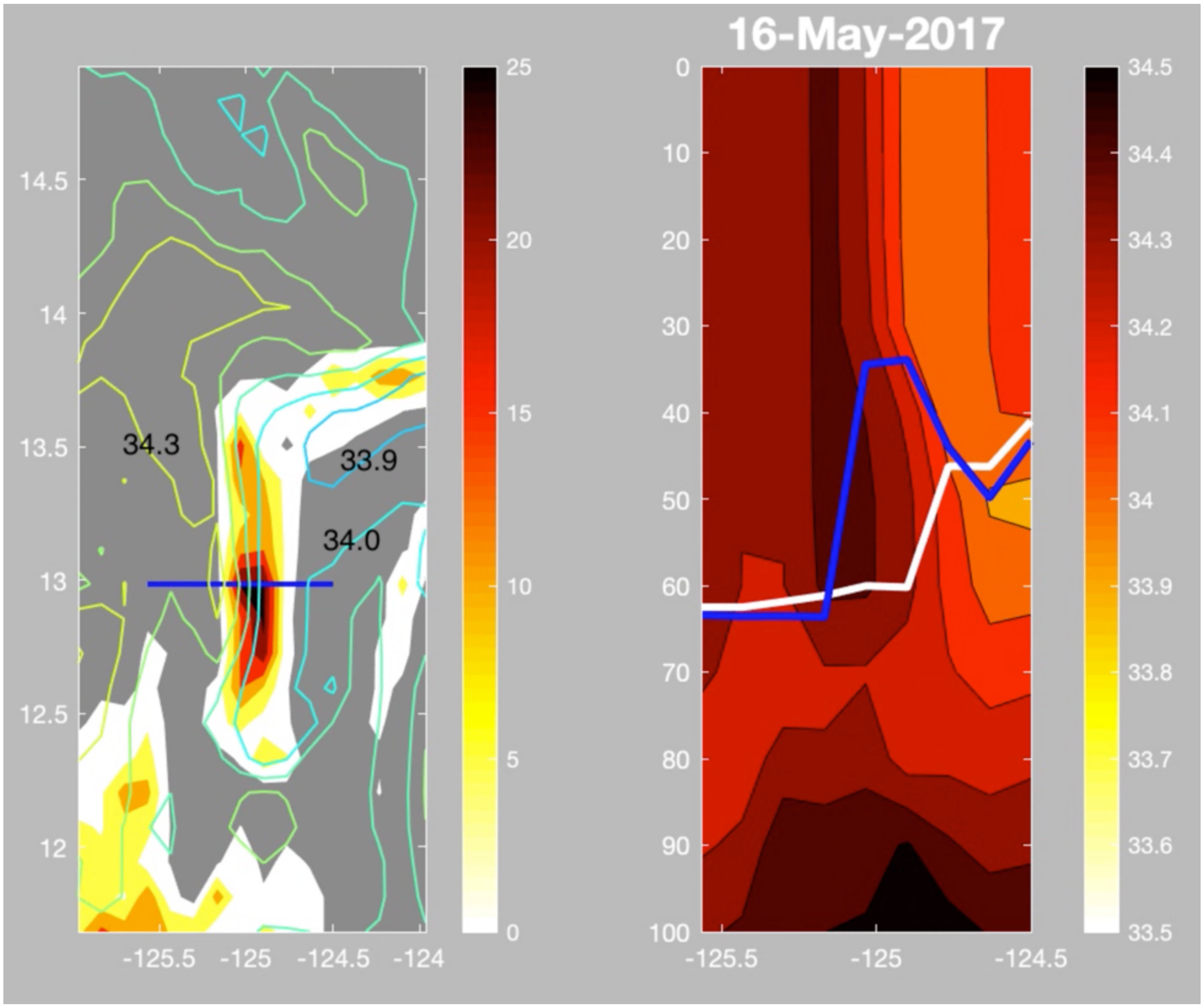

Figure 10. BLT and salinity on 16 May 2017 extracted from Animation S2. Left panel: Colored contours: SSS with contour interval 0.1. High SSS in yellow and low SSS in blue. Colors: BLT with color scale at right. Grey color indicates zero BLT. Blue line is the location of the vertical section displayed in the right panel. x-axis is longitude (°E), y-axis latitude (°N). Right panel:

Vertical salinity section across the front in the left panel, with depth in meters and longitude in °E. Blue line is the MLD. White line is the ILD. The difference between them is the BLT.

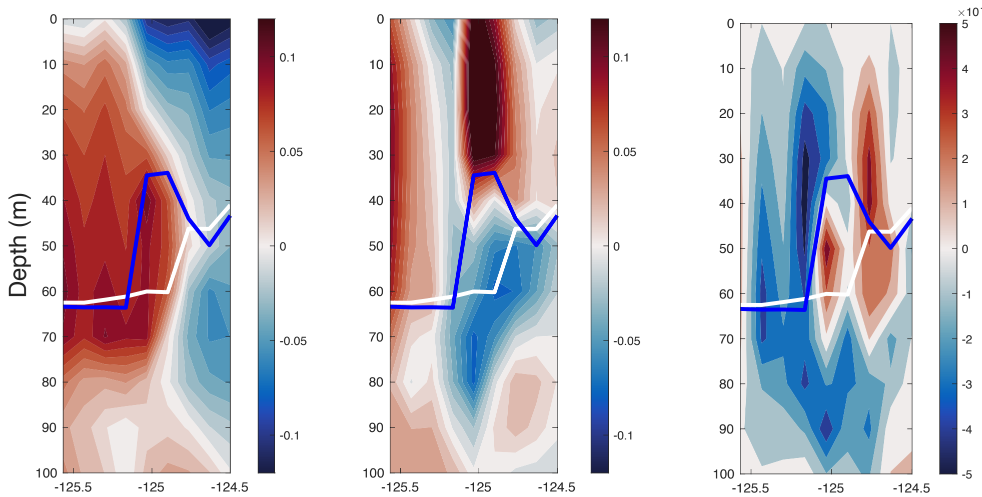

(a) (b) (c)

Figure 11. a) Zonal velocity (m/s) along the same section as in Figure 10 right panel for 16 May 2017. White line is the ILD and blue line is the MLD. Red (blue) colors indicate positive (negative) velocity, or to the left (right) in the section. b) Same as panel a), but for meridional velocity. Red (blue) colors indicate flow northward or into the page (southward or out of the page) c) Same as panel a) but for vertical velocity. Upward flow in red colors, downward in blue.

4 Summary and Discussion

Using a version of ROMS set up for the SPURS-2 region in the eastern tropical Pacific Ocean, we have studied two events when BLs appeared in the model. Both events were associated with sharp mixed layer salinity fronts. The first occurred at 6-7°N in October 2017, the other occurred at 12-13°N in May 2017, at the leading edge of the extension of the EPFP. In each case, a thick BL was created when the bottom part of a salinity front tilted towards the fresh side of the front. In the October event, the formation of the BL was associated with spreading of fresh water over the salty water and motion of the salinity front. In the May 2017 event, the front remained relatively stationary, and persisted for more than two weeks.

The hypothesis of KS20 and CM02 is that BLs can be formed by tilting of vertically-oriented isohalines by shear flow at a mixed layer salinity front. The analysis of the May and October 2017 events suggests a modified version of this mechanism (Figure 11) that the full concurrent property and velocity fields from the model simulation enable us to better resolve compared to the *in situ* observations. This starts with a vertical front of salinity in the mixed layer. On the fresh side of the front the flow is horizontally divergent at the surface, and pulls water up from the mixed-layer base. On the salty side of the front, the flow is convergent at the surface, and pushes water down into the mixed layer. The opposite is the case at the base of the mixed layer, with divergence on the salty side and convergence on the fresh side. Thus, a small vertical circulation cell is set up with water flowing across the front at the mixed layer base from the salty to the fresh side. At the base of the mixed layer, the isohalines then tilt generating the BL that is observed. The mixed layer front is accompanied by a strong vertical shear through the thermal wind relation. This vertical shear may play a role in generating and maintaining the horizontal convergences and divergences that drive the vertical circulation (KS20). In particular, the surface divergence on the fresh side of the front may be due to acceleration of the flow by concentration of the front's isohalines at the location of the BL (Figure 11b).

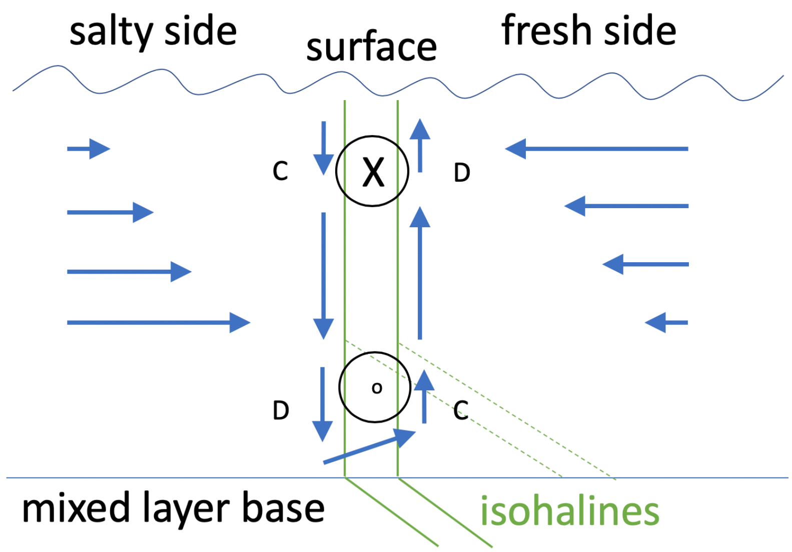

Figure 12. Schematic view of proposed BL formation mechanism in the ETP showing a section across a zonal salinity front in the mixed layer as in Figure 10b. The zonal velocity, the arrows at the left and right, indicate a tilting shear flow. On the salty side of the front there is horizontally convergent flow at the surface and divergent flow at the base of the mixed layer. By contrast, on the fresh side there is divergent flow at the surface and convergent flow at the base of the mixed layer. This sets up a vertical circulation that acts to tilt isohalines mainly at the front's base (dashed lines) and generate a thick BL. Included is a strong vertical shear parallel to the front (into/out of the page) which helps to maintain the vertical orientation of the front at the surface and contribute to the convergent and divergent parts of the flow.

The proposed mechanism shown in Figure 12 is two-dimensional. However, this greatly simplifies the surface circulation in reality that generates and moves the front and associated convergence/divergence and ignores mixing and entrainment of salt through the base of the mixed layer. The schematic does however, place emphasis on vertical processes in the vicinity of a front, which seems appropriate given the apparent association between BL formation, horizontal divergence and the presence of fronts (KS20). Indeed, Vialard and Delecluse (1998b) suggest a similar mechanism, including downwelling near the front, but emphasize the role of precipitation to a greater degree. That study was conducted in the western tropical Pacific where precipitation may be more important in the BL formation process.

KS20 emphasize the importance of Ekman transport in the formation of BLs, especially in summer and fall in the eastern tropical North Pacific. We note that formation of thick BLs in the October 2017 event is associated with a sudden relaxation of the winds between 26 and 27-October (Figure 6). There is no indication that the currents slowed or stopped as a result of this

(Figure 3). However, the disturbance in the wind forcing may have been enough to produce submesoscale eddies and a growing set of convergences and divergences at the surface (Figure 4) that were able to generate fronts and BLs during October 2017 (see also Animation S1, 18-31-October-2017).

Tanguy et al. (2007) discuss the diversity of situations and causes responsible for the BLs observed in the tropical Atlantic. Some instances of BLs arise in similar ways to those depicted here in the ETP, on the fresh side of a mixed layer salinity front and at the front's base (see Tanguy et al (2007) their Figures 10c, e and f). As noted above, it has been hypothesized that BLs act to insulate the full mixed layer from surface buoyancy flux and entrainment cooling from below (Godfrey and Lindstrom, 1989; Vialard and Delecluse, 1998a) and concentrate heating into the upper part of the mixed layer. If this is the case, then it follows that in the tropics, as these BLs are formed, heating preferentially occurs on the fresh sides of submesoscale fronts. As the mixed layer is heated in that region, the density contrast across the front is enhanced, along with the lifetime of the front. This may be why these fronts can last for long periods of time, such as the one in the Animation S2 which lasts more than two weeks, despite the fact that they are unstable.

In this work, we have analyzed two very limited appearances of BLs, and attributed certain characteristics to them. This is not to say that all, or even most, BLs in the ETP necessarily follow this script. However, given the ubiquity of these features as seen in Animation S1 and documented by KS20, there is no doubt the BLs introduce variance into the processes of entrainment at the base of the mixed layer and the flux of heat and fresh water across the surface. This variance itself may help to generate the submesoscale flows that create fronts and in turn work to increase variance in salinity, a positive feedback loop. This positive feedback, acting on the large scale salinity field can perhaps lead to or accelerate the extension of the surface salinity minimum that stretches across the tropical Pacific (Melnichenko et al., 2019).

Acknowledgments and Data

Color scales for all color figures were taken from the "cmocean" package (Thyng et al., 2016).

There are no known financial conflicts of interest on the parts of the authors of this paper, neither are there any unstated affiliations among the authors that could be perceived as a conflict of interest.

SPURS-2 central mooring data can be accessed here:

- http://dx.doi.org/10.5067/SPUR2-MOOR1

The authors express their appreciation to J. T. Farrar for providing this high quality dataset.

SPURS-2 uCTD data can be accessed here:

- http://dx.doi.org/10.5067/SPUR2-UCTD0

ROMS output can be accessed here:

- [add location here].

FB's work on SPURS-2 is supported by NASA grant NNX15AF72G, and by the Jet Propulsion Laboratory through the Salinity Continuity Processing activity. SK is supported the Japan

Society for the Promotion of Science (JSPS) under its Overseas Research Fellowships program. JS and SK are supported by NASA Grant Number 80NSSC18K1500.

References

Alory, G., C. Maes, T. Delcroix, N. Reul, and S. C. C. Illig (2012), Seasonal dynamics of sea surface salinity off Panama: The far Eastern Pacific Fresh Pool, Journal of Geophysical Research, 117(C4), C04028, doi:10.1029/2011JC007802.

Cronin, M. F., and M. J. McPhaden (2002), Barrier layer formation during westerly wind bursts, Journal of Geophysical Research: Oceans, 107(C12), doi:10.1029/2001JC001171.

de Boyer Montegut, C., J. Mignot, A. Lazar, and S. Cravatte (2007), Control of Salinity on the Mixed layer depth over the world ocean: 1. General Description, Journal of Geophysical Research, C112, 6011, doi:10.1029/2006JC003953.

Fairall, C. W., E. F. Bradley, J. Hare, A. A. Grachev, and J. B. Edson (2003), Bulk parameterization on air–sea fluxes: Updates and verification for the COARE algorithm, Journal of Climate, 16, 571-591.

Farrar, J. T. (2019), SPURS-2 Central mooring CTD, surface flux and meterorological data for the E. Tropical Pacific field campaign, NASA/JPL/PO.DAAC, Pasadena, CA, doi:10.5067/SPUR2-MOOR1.

Farrar, J. T., and A. J. Plueddemann (2019), On the Factors Driving Upper-Ocean Salinity Variability at the Western Edge of the Eastern Pacific Fresh Pool, Oceanography, 32, doi:10.5670/oceanog.2019.209.

Fiedler, P. C., and L. D. Talley (2006), Hydrography of the eastern tropical Pacific: A review, Progress in Oceanography, 69(2), 143-180, doi:10.1016/j.pocean.2006.03.008.

Godfrey, J. S., and E. J. Lindstrom (1989), The heat budget of the equatorial western Pacific surface mixed layer, Journal of Geophysical Research: Oceans, 94(C6), 8007-8017, doi:10.1029/JC094iC06p08007.

Good, S. A., M. J. Martin, and N. A. Rayner (2013), EN4: Quality controlled ocean temperature and salinity profiles and monthly objective analyses with uncertainty estimates, Journal of Geophysical Research: Oceans, 118(12), 6704-6716, doi:10.1002/2013JC009067.

Guimbard, S., N. Reul, B. Chapron, M. Umbert, and C. Maes (2017), Seasonal and interannual variability of the Eastern Tropical Pacific Fresh Pool, Journal of Geophysical Research: Oceans, 122(3), 1749-1771, doi:10.1002/2016JC012130.

Katsura, S., E. Oka, and K. Sato (2015), Formation Mechanism of Barrier Layer in the Subtropical Pacific, Journal of Physical Oceanography, 45(11), 2790-2805, doi:10.1175/JPO-D-15-0028.1.

Katsura, S., and J. Sprintall (2020), Seasonality and Formation of Barrier Layers and Associated Temperature Inversions in the Eastern Tropical North Pacific, Journal of Physical Oceanography, 50(3), 791-808, doi:10.1175/JPO-D-19-0194.1.

Katsura, S., J. Sprintall, and F. M. Bingham (2020), Upper Ocean Stratification in the Eastern Pacific during the SPURS-2 Field Campaign, Journal of Geophysical Research Oceans, Submitted.

Li, Z., F. M. Bingham, and P. P. Li (2019), Multiscale Simulation, Data Assimilation, and Forecasting in Support of the SPURS-2 Field Campaign, Oceanography, 32, doi:10.5670/oceanog.2019.221.

Li, Z., J. C. McWilliams, K. Ide, and J. D. Farrara (2015), A Multiscale Variational Data Assimilation Scheme: Formulation and Illustration, Monthly Weather Review, 143(9), 3804-3822, doi:10.1175/MWR-D-14-00384.1.

Lindstrom, E., J., J. B. Edson, J. J. Schanze, and A. Y. Shcherbina (2019), SPURS-2: Salinity Processes in the Upper-Ocean Regional Study 2 – The Eastern Equatorial Pacific Experiment, Oceanography, 32, doi:10.5670/oceanog.2019.207.

Lukas, R., and E. Lindstrom (1991), The Mixed Layer of the Western Equatorial Pacific, Journal of Geophysical Research, 96 (suppl.), 3343-3357, doi:10.1029/90JC01951.

Maes, C., J. Picaut, and S. Belamari (2002), Salinity barrier layer and onset of El Niño in a Pacific coupled model, Geophysical Research Letters, 29(24), 59-51-59-54, doi:10.1029/2002GL016029.

Maes, C., J. Picaut, and S. Belamari (2005), Importance of the Salinity Barrier Layer for the Buildup of El Niño, Journal of Climate, 18(1), 104-118, doi:10.1175/JCLI-3214.1.

Melnichenko, O., P. Hacker, F. M. Bingham, and T. Lee (2019), Patterns of SSS Variability in the Eastern Tropical Pacific: Intraseasonal to Interannual Timescales from Seven Years of NASA Satellite Data, Oceanography, 32, doi:10.5670/oceanog.2019.208.

Pujol, M. I., Y. Faugère, G. Taburet, S. Dupuy, C. Pelloquin, M. Ablain, and N. Picot (2016), DUACS DT2014: the new multi-mission altimeter data set reprocessed over 20 years, Ocean Sci., 12(5), 1067-1090, doi:10.5194/os-12-1067-2016.

Roemmich, D., M. Morris, W. R. Young, and J. R. Donguy (1994), Fresh Equatorial Jets, Journal of Physical Oceanography, 24(3), 540-558, doi:10.1175/1520-0485(1994)024<0540:FEJ>2.0.CO;2.

Sato, K., T. Suga, and K. Hanawa (2004), Barrier layer in the North Pacific subtropical gyre, Geophysical Research Letters, 31, 5301, doi:5310.1029/2003GL018590.

Sato, K., T. Suga, and K. Hanawa (2006), Barrier layers in the subtropical gyres of the world's oceans, Geophysical Research Letters, 33, L08603, doi:10.1029/2005GL025631.

Schanze, J. J., R. W. Schmitt, and L. L. Yu (2010), The global oceanic freshwater cycle: A state-of-the-art quantification, Journal of Marine Research, 68(3-1), 569-595, doi:10.1357/002224010794657164.

Shchepetkin, A. F. and J. C. McWilliams, J. C. (2011). Accurate Boussinesq oceanic modeling with a practical, stiffened equation of state. *Ocean Modell*., 38, 41–70.

Sprintall, J., and M. Tomczak (1992), Evidence for the Barrier Layer in the Surface layer of the Tropics, Jour. Geophys. Res. C Oceans, 97, 7305-7316, doi:10.1029/92JC00407.

Sprintall, J. (2019a), SPURS-2 research vessel Underway CTD (uCTD) data for the E. Tropical Pacific R/V Revelle cruises. Ver. 1.0. PO.DAAC, CA, USA. Dataset accessed 2020-07-21 at doi:10.5067/SPUR2-UCTD0**.**

Sprintall, J. (2019b), Upper ocean salinity stratification during SPURS-2. Oceanography 32(2):40 - 41, doi:10.5670/oceanog.2019.210.

Tanguy, Y., S. Arnault, and P. Lattes (2010), Isothermal, mixed, and barrier layers in the subtropical and tropical Atlantic Ocean during the ARAMIS experiment, Deep Sea Research Part I: Oceanographic Research Papers, 57(4), 501-517, doi:10.1016/j.dsr.2009.12.012.

Thyng, K. M., C. A. Greene, R. D. Hetland, H. M. Zimmerle, and S. F. DiMarco (2016), True Colors of Oceanography: Guidelines for Effective and Accurate Colormap Selection, Oceanography, 29(3), 9-13, doi:10.5670/oceanog.2016.66.

Veneziani, M., A. Griffa, Z. Garraffo, and J. A. Mensa (2014), Barrier Layers in the Tropical South Atlantic: Mean Dynamics and Submesoscale Effects, Journal of Physical Oceanography, 44(1), 265-288, doi:10.1175/JPO-D-13-064.1.

Vialard, J., and P. Delecluse (1998a), An OGCM Study for the TOGA Decade. Part I: Role of Salinity in the Physics of the Western Pacific Fresh Pool, Journal of Physical Oceanography, 28(6), 1071-1088, doi:10.1175/1520-0485(1998)028<1071:AOSFTT>2.0.CO;2.

Vialard, J., and P. Delecluse (1998b), An OGCM Study for the TOGA Decade. Part II: Barrier-layer Formation and Variability, J. Phys. Oceanogr., 28(6), 1089-1106, doi:10.1175/1520-0485(1998)028%3C1089:AOSFTT%3E2.0.CO;2.

Yu, L. (2015), Sea-surface salinity fronts and associated salinity-minimum zones in the tropical ocean, Journal of Geophysical Research Oceans, 120, 4205–4225, doi:10.1002/2015JC010790.